

## Image Deblurring using $L_0$ Sparse and Directional Filters

**Aparna Ashok**

*Department of Electronics and Communication Engineering  
Mar Baselios College of Engineering and Technology  
Trivandrum, India.*

*aparnaashok1988@gmail.com*

**Deepa P. L.**

*Department of Electronics and Communication Engineering  
Mar Baselios College of Engineering and Technology  
Trivandrum, India.*

*deeparahul2022@gmail.com*

---

### Abstract

Blind deconvolution refers to the process of recovering the original image from the blurred image when the blur kernel is unknown. This is an ill-posed problem which requires regularization to solve. The naive MAP approach for solving the blind deconvolution problem was found to favour no-blur solution which in turn led to its failure. It is noted that the success of the further developed successful MAP based deblurring methods is due to the intermediate steps in between, which produces an image containing only salient image structures. This intermediate image is essentially called the unnatural representation of the image.  $L_0$  sparse expression can be used as the regularization term to effectively develop an efficient optimization method that generates unnatural representation of an image for kernel estimation. Further, the standard deblurring methods are affected by the presence of image noise. A directional filter incorporated as an initial step to the deblurring process makes the method efficient to be used for blurry as well as noisy images. Directional filtering along with  $L_0$  sparse regularization gives a good kernel estimate in spite of the image being noisy. In the final image restoration step, a method to give a better result with lesser artifacts is incorporated. Experimental results show that the proposed method recovers a good quality image from a blurry and noisy image.

**Keywords:** Motion Blur, Blind Deconvolution, Deblurring,  $L_0$  Sparsity, Directional Filtering, Image Restoration.

---

### 1. INTRODUCTION

Motion blur caused by camera shake is the most common artifact and one of the predominant source of degradation in digital photography. Photos taken in low light without flash requires higher exposure times and thereby the photos get affected by motion blur. Increasing the light sensitivity of the camera using a higher ISO setting may help in reducing the exposure time, but there is a trade off with noise levels. The lower exposure time comes at the cost of higher noise levels. Even then, the exposure time still remains high for handheld photography and camera shake is likely to happen without the use of a tripod. As a result, the photos end up being blurry and noisy. Recovering an unblurred, sharp image from a single motion blurred image is one of the major research areas in digital photography. This problem can be further divided into blind and non-blind cases. If the blur kernel that has degraded the image is known, then the only problem is the estimation of the unknown latent image by the deconvolution process. This is referred non-blind deblurring. If there is no information available about the kernel that has degraded the image, the original image has to be estimated from the blurred image using the mathematical model of the blurring process. The kernel and the image has to be estimated simultaneously and iteratively in this process. This is a much more ill-posed task and is referred to as blind deblurring. A large number of techniques have been proposed in the recent times to address the problem of blind image deblurring, by jointly estimating the latent deblurred image

while recovering the blur kernel which has degraded the image. Most of these methods assume an ideal condition with little image noise and demonstrates a fair level of success in such photos. However a significant amount of noise affect the performance of the existing standard blind deblurring algorithms. The presence of noise causes high frequency perturbations of the image values and this is not taken into consideration by the standard blind deblurring methods. In the blind deblurring process, the image noise manifests itself as noise in the estimated kernel and is further amplified by the deconvolution process. This produces artifacts in the deblurring result.

Single image blind deconvolution was extensively studied in the recent years and the field has reached considerable success with many milestones. The basic concept of blind deconvolution and different existing types of blind deconvolution algorithms are explained in detail by D. Kundur and D. Hatzinakos in their paper [1]. The classifications of blind deconvolution techniques are explained and its merits and demerits are discussed. MAP method is the most commonly used among the blind deblurring techniques because it does not require any a priori information about the PSF and also, it does not constrain the PSF to be of any specific parametric form. Naive MAP approach was seen to fail on natural images as it tends to favor no blur solution. Levin et al.[2] analyzed the source of MAP failure and demonstrated that marginalizing the process over the image  $x$  and MAP estimation of the kernel  $k$  alone proves successful and recovers an accurate kernel. As noted by Levin et al.[2] and Fergus et al.[3], blurry images have a lower cost compared to sharp images in MAP approach and as a result blurry images are favored. So, a number of more complex methods have been proposed that include marginalization over all possible images[2,3], dynamic adaptation of the cost function used[4],determining edge positions by the usage of shock filtering[5] and reweighting of image edges during optimization[6]. Many papers emphasized the usage of sparse prior in derivative domain to favor sharp images. But expected result has not been yielded by the direct application of this principle, as it required additional processes like marginalization across all possible images as demonstrated by Fergus et al.[3] spatially varying terms or solvers that vary optimization energy over time as shown by Shan et al.[4].Krishnan et al.[7] used  $l_1/l_2$  norm as the sparsity measure which acts as a scale invariant regularizer. Xu et al.[8] introduced  $L_0$  sparsity as regularization term ,which relies on the intermediate representation of image for its success. All of the mentioned deblurring methods generally work well when the image is noise free, but their performance deteriorates in the presence of noise, as the noise level increases[3,9,10]. It has been noticed that standard denoising methods like Wiener filtering, NLM filtering have negative effect on the kernel estimation process[11,12]. Zhong et al.[13] proposed an approach based on directional filtering followed by Radon transform for accurate kernel estimation in the presence of noise.

This paper proposes a new blind deconvolution algorithm for the deblurring of blurry and noisy images using  $L_0$  sparse prior, which is equipped with appropriate noise handling using directional filters, and a method incorporated in final image restoration step to obtain a good quality latent image with lesser artifacts. It has been noted that the prior MAP based approaches that are successful can be roughly classified into two types i.e. those with explicit edge prediction steps like using a shock filter [5,6,14,15,16,17,18,19] and those which include implicit regularization process[7,8]. The common factor in these two is that they both include an intermediate step, which produces an image which contains only the salient structures while suppressing others. This intermediate image which contains only step like or high contrast structures is called the unnatural representation of the image. These image maps are the key for making motion deblurring process accomplishable in different successful MAP based methods. The  $L_0$  sparse prior acts as a regularization term and enables accurate kernel estimation through the unnatural representation of the image. Directional filters are seen to remove noise in an image effectively, without affecting the blur kernel estimation process in a significant manner. Consequently, directional filters can be successfully incorporated in the deblurring technique for noise handling, without the problem of steering kernel estimation along the wrong direction. The incorporation of an additional process for reducing the artifacts while enhancing finer details ensures a good quality latent image.

## 2. PROPOSED WORK

Directional lowpass filters can be applied to an image to reduce its noise level without tampering with the process of kernel estimation on a significant level. The application of directional lowpass filter  $h_\theta$  to an image  $I$  can be explained theoretically by the equation

$$I(p) * h_\theta = \frac{1}{r} \int_{-\infty}^{\infty} w(t) I(p + tu_\theta) dt \quad (1)$$

where  $p$  denotes the location of each pixel,  $r$  is the normalization factor given as  $r = \int_{-\infty}^{\infty} w(t) dt$ ,  $t$  is the spatial distance from each pixel to  $p$  and  $u_\theta$  is the unit vector in the direction of application of the filter,  $\theta$ . We choose the directional filter to have a Gaussian profile and this is determined by the factor  $w(t)$  which can be given by the expression  $w(t) = e^{-t^2/2\sigma^2}$  where  $\sigma$  is the factor which controls the strength of the Gaussian directional filtering process[20].

The image, after the directional filtering process, is to be now advanced to the kernel estimation step for the blind deblurring process. A regularization term which consists of a family of loss functions, that approximates  $L_0$  cost, is incorporated into the objective function which has to be optimized.  $L_0$  approximation enables a high sparsity pursuit regularization, which also leads to consistent energy minimization and fast convergence during the optimization process. Since only the salient structures of the image are retained in the unnatural representation, the method is faster than other implicit regularization methods. This family of loss functions that approximates  $L_0$  cost implements graduate non-convexity into the optimization process and the significant edges guides the kernel estimation process in the right direction, thus quickly improving the estimation process in only a few iterations.

The image that has been obtained at the end of kernel estimation step is not our required latent image due to the lack of details, as it contains just high contrast edges. A final image restoration step has to be carried out for obtaining the latent image. An existing non-blind deconvolution can be used for this. From the study of the existing non-blind deblurring methods, it can be seen that non-blind deblurring using Laplacian prior shows a great preservation of finer details[21]. But at the same time, the result is seen to have considerably significant artifacts in the case of Laplacian prior. On the contrary, a restoration step using  $L_0$  prior produces image with very less artifacts though the finer details are fewer[22]. Therefore, instead of simply performing non-blind deconvolution with the obtained kernel using hyper Laplacian prior, a simple method is proposed to get a latent image with finer details and fewer artifacts. First, latent image  $I_1$  is estimated using the non-blind deconvolution method with hyper-Laplacian prior. After this, latent image  $I_0$  is estimated using the  $L_0$  prior scheme introduced in our paper. The difference map of these two estimated images is computed, followed by bilateral filtering to remove artifacts in the difference map obtained. Subtracting the result of bilateral filtering from  $I_1$  gives the desired final image output which contains finer details with fewer artifacts.

## 3. MATHEMATICAL FRAMEWORK

We denote the latent image by  $x$ , blurred and noisy image by  $y$  and the blur kernel by  $k$ . The blurring process can be represented generally as

$$y = k * x + \eta \quad (2)$$

where  $\eta$  represents the image noise. The blurred and noisy image  $y$  has to be first of all denoised, by the application of directional low pass filters with Gaussian profile in the desired orientations. The strength of the filtering process by directional filter  $h_\theta$  along each orientation  $\theta$  is denoted by its  $\sigma$  value. This value can be decided accordingly based on the image at hand and the noise infected along that particular direction. After deciding on the different orientations for the application of directional filters and the strength of Gaussian profile filtering along each direction,

denoising is carried out. This gives a noise-free image without affecting the blur of the image considerably in a way that will interfere with accurate kernel estimation.

The framework of the proposed deblurring technique includes a loss function  $\Phi_0(\cdot)$  that approximates  $L_0$  cost into the objective function during optimization process. The loss function for an image  $z$  can be defined as

$$\Phi_0(\partial_* z) = \sum_i \Phi(\partial_* z_i) \tag{3}$$

where,

$$\Phi(\partial_* z_i) = \begin{cases} \frac{1}{\varepsilon^2} |\partial_* z_i|^2, & \text{if } |\partial_* z_i| \leq \varepsilon \\ 1 & \text{otherwise} \end{cases} \tag{4}$$

and  $* \in \{h, v\}$  denoting the horizontal and vertical directions respectively for each pixel  $i$ , for taking gradient of the image. This function is continuous when  $|\partial_* z_i| \leq \varepsilon$ , which is a necessary condition for being a loss function mathematically. This loss function is a very high sparsity pursuit one that approximates sparse  $L_0$  function very closely.

The final objective function is obtained by incorporating the loss function  $\Phi_0(\cdot)$  in our method as a regularization term during the optimization process, which in turn seeks an intermediate sparse representation of the image containing only salient edges, which guides the kernel estimation in the right direction. The objective function for kernel estimation can be given as

$$\min_{(\tilde{x}, k)} \{ \|k * \tilde{x} - y\|^2 + \lambda \sum_{* \in \{h, v\}} \Phi_0(\partial_* \tilde{x}) + \gamma \|k\|^2 \} \tag{5}$$

where  $\tilde{x}$  is the unnatural representation of the image during the process of optimization of the objective function and  $\lambda, \gamma$  are regularization weights. The first term of the objective function is the data fidelity term which enforces blur model constraint, second term is the loss function approximating sparse  $L_0$  and the last term helps in reducing the kernel noise. It can be seen that the new regularization term is the key factor in guiding the kernel estimation process quickly and accurately in the right direction. If we consider the case of explicit edge prediction methods like employing a shock filter, it cannot be incorporated into the objective function during the optimization process. But the advantage in the case of using the  $L_0$  sparse regularization term is that, it can be efficiently incorporated into the objective function during the optimization process, which ensures the fact that the intermediate representation of the image contains only necessary strong edges that satisfy the constraints, regardless of the blur kernel.

The objective function can be solved by alternatively computing the intermediate image value and the kernel value in each iteration[23]. The computation process for  $(t+1)^{\text{th}}$  iteration of optimization process can be given by Eq. 6 and Eq. 7.

$$\tilde{x}^{t+1} = \underset{\tilde{x}}{\operatorname{argmin}} \left\{ \|k^t * \tilde{x} - y\|^2 + \lambda \sum_{* \in \{h, v\}} \Phi_0(\partial_* \tilde{x}) \right\} \tag{6}$$

$$k^{t+1} = \underset{k}{\operatorname{argmin}} \{ \|\tilde{x}^{t+1} * k - y\|^2 + \gamma \|k\|^2 \} \tag{7}$$

Equation 4 for the loss function can be rewritten as follows with  $\varepsilon$  as a parameter, for the ease of the optimization process.

$$\Phi(\partial_* z_i, \varepsilon) = \min_{l_{*i}} \left\{ |l_{*i}|^0 + \frac{1}{\varepsilon^2} (\partial_* z_i - l_{*i})^2 \right\} \tag{8}$$

where,  $*$   $\in$  { h, v } and

$$l_{*i} = \begin{cases} 0 & , |\partial_{*}\tilde{x}_i| \leq \epsilon \\ \partial_{*}\tilde{x}_i & , \text{otherwise} \end{cases} \quad (9)$$

The above function can be proved to be mathematically equivalent to the previous one. A family of loss functions are obtained based on this equation by setting the value of  $\epsilon$  differently. Figure 1 shows the family of loss functions for different values of  $\epsilon$  starting from 1 to 1/8 and the plot approaches  $L_0$  further as the value of  $\epsilon$  keeps on decreasing.

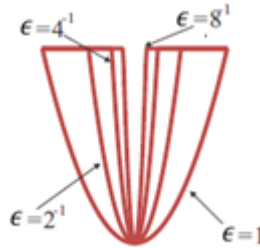


**FIGURE 1:** Plots of the loss function approximating  $L_0$  for different values of  $\epsilon$ .

Equation 6 for the optimization process computing  $\tilde{x}$  can also be rewritten accordingly based on Eq.8 and Eq.9 .

$$\min_{\tilde{x}, l} \left\{ \frac{1}{\lambda} \|k * \tilde{x} - y\|^2 + \sum_{* \in \{h,v\}} \sum_i \{ |l_{*i}|^0 + \frac{1}{\epsilon^2} (\partial_{*}\tilde{x}_i - l_{*i})^2 \} \right\} \quad (10)$$

We alternate the process of computing intermediate image  $\tilde{x}$  and updating the value of  $l_{*i}$  in the iterations for each of the loss function obtained for different values of  $\epsilon$ . The whole optimization process can be speeded up by transforming the computation process into FFT domain. Using FFTs with the quadratic form enables fast kernel estimation process. The solution in FFT domain can be expressed by Eq.11 and Eq. 12.

$$\tilde{x}^{t+1} = F^{-1} \left\{ \frac{\overline{F(k^t)} \cdot F(y) + \frac{\lambda}{\epsilon^2} (\overline{F(\partial_h)} \cdot F(l_h) + \overline{F(\partial_v)} \cdot F(l_v))}{\overline{F(k^t)} \cdot F(k^t) + \frac{\lambda}{\epsilon^2} (|F(\partial_h)|^2 + |F(\partial_v)|^2)} \right\} \quad (11)$$

$$k^{t+1} = F^{-1} \left\{ \frac{F(\tilde{x}^{t+1}) \cdot F(y)}{|F(\tilde{x}^{t+1})|^2 + \gamma} \right\} \quad (12)$$

where,  $F(\cdot)$  and  $\overline{F(\cdot)}$  are the FFT operator and its conjugate respectively,  $F^{-1}$  is the inverse FFT operation whereas  $\cdot$  and  $\overline{\cdot}$  are vectors concatenating and values for each pixel.  $F_D^2$  denotes  $|F(\partial_h)|^2 + |F(\partial_v)|^2$ . Multiplication and division operations are performed in an element wise manner on the complex vectors.

During the implementation process, we use a family of 4 loss functions with  $\epsilon \in \{1, 1/2, 1/4, 1/8\}$ . We start from  $\epsilon = 1$  and then proceed to the other values as shown in Figure 1. The number of iterations for different loss functions is set to be inversely proportional to the corresponding value of  $\epsilon$ . This is because of the fact that large  $\epsilon$  values cause the loss function to be more convex like

and hence makes it more easy to optimize. So it requires only a few iterations. The results obtained here is taken as an initialization for further refinement in loss functions with smaller  $\epsilon$  values, as they are of more concave nature and difficult to optimize. Also, the blur kernel estimation process is carried out in a pyramid-like fashion, by convention. Kernels are estimated in a coarse to fine manner in an image pyramid. The estimate obtained in one image pyramid level is taken as the initialization of the next one. The optimization process in each iteration  $t+1$  in its finest level is as explained by the equations Eq.11 and Eq.12 .Computation is similar in the coarser level for different iterations.

The algorithm for kernel estimation process in one image level can be given as follows

Input: Blurry and noisy image  $y$

Output: Blur kernel  $k$ , deblurred image  $\tilde{x}$

- 1 Apply  $N$  directional filters to the input image  $y$ , where each filter has a direction given by the expression  $\theta=(i.\pi/N), i=1,2,\dots,N$  and  $N$  is the number of directional filters. Choose the  $\sigma$  value for each direction accordingly depending on the image.
- 2 Initialize  $k$  from the kernel estimate of coarser scale
- 3 for  $t= 1:5$ 
  - 4 //update image
  - 5  $\epsilon \rightarrow 1$
  - 6 for  $i=1:4$ 
    - 7 for  $j=1: \epsilon^{-1}$ 
      - 8 solve for  $l$  using equation (9)
      - 9 solve for  $\tilde{x}^{t+1}$  using equation (11)
    - 10 end
    - 11  $\epsilon \rightarrow \epsilon/2$
  - 12 end
  - 13 //update kernel
  - 14 solve for  $k^{t+1}$  using equation (12)
- 15 end

Desired kernel estimate is obtained at the end of algorithm execution for each image level, in a coarse to fine manner. Five iterations of alternative image and kernel estimation are required generally at each level. But the computed image  $\tilde{x}$  at the end of the algorithm is not the final latent image because it contains only salient edges and lacks details. A non-blind deconvolution using hyper Laplacian prior can be used for latent image restoration in general case. But here, we go for a better method to remove artifacts and obtain a much better quality image. We take advantage of the fact that non-blind deconvolution with hyper Laplacian prior produces an image result with very fine details but a considerable amount of artifacts, whereas restoration using  $L_0$  prior and the estimated kernel produces a result with very less artifacts though the result may not contain much finer details. A difference map between these two results is computed and it is

subjected to bilateral filtering. Further subtraction of the obtained filtered result from the result of non-blind deconvolution with hyper Laplacian prior produces a latent image with finer details and practically very less artifacts. It can be seen that this results in a much better quality result when compared to the result that would have been produced if we had gone for a normal non-blind deconvolution using estimated kernel obtained in the previous step. The latent image restoration step can also be accelerated by the use of FFT.

#### 4. EXPERIMENTAL RESULTS

We experiment with data on different natural and synthetic images blurred by a set of 8 different blur kernels. We implemented the proposed method in Matlab on an Intel Core i7 CPU. The value of parameters are set to  $\lambda=2e-3$  and  $\gamma = 40$  for all experiments. Initially, we test the algorithm for images affected by just blurring by excluding the directional filtering part from our experimental process i.e. we estimate the kernel by L0 prior scheme and then use the method explained in the paper for latent image restoration along with artifacts removal. After that, we take blurry and noisy images and carry out the entire experimental process starting with directional filtering. Gaussian random noise with a sigma value of 7 has been used in our experiments. We applied directional filters along 24 regularly sampled directions i.e. one sample every  $15^\circ$ . We have taken  $\sigma$  value of the filter to be 1 or 2 depending on the image and we have tested with the same  $\sigma$  value in all directions, though this can be varied for different directions if the image demands so. It can be seen that the final images in the case without noise are of excellent visual quality and shows a high improvement in PSNR values. Further, in the case of blurry and noisy images, the process produces a good visual quality image in spite of the presence of noise, unlike standard deblurring algorithms that produce deteriorated results in the presence of noise. Comparative studies have been performed with standard existing methods of deblurring and denoising. The results obtained using directional filtering for noise removal process can be found superior to the one obtained using Wiener filter, which has been the most commonly used filtering method in image processing field in the recent times.

First of all, experimental results obtained on simulation with a blurry image is shown to demonstrate the process. Fig. 2 shows the comparison of results between our method and the method proposed by Xu et al. [8] which has a standard non-blind deconvolution step using hyper-Laplacian priors [21]. The intermediate step which is the unnatural representation of the image, the estimated kernel, latent image restored in the case of non-blind deconvolution applied directly [8], latent image restored by our method including a simple artifact removing step (and excluding directional filtering step) are shown in the figure. It can be seen that latent image restored by our method is of clearly of much better visual quality and even has a higher PSNR value compared to the results produced by Xu et al. [8]. Some more results of our method (excluding directional filtering) on blurry images are shown in Fig. 3 which shows the blurry image, restored latent image and estimated kernel. The method clearly restores an excellent visual quality image.



(a)blurry input.

(b)unnatural representation and estimated kernel.



(c)Restored latent image for  
Xu et al.[8].  
PSNR= 28.52

(d) our restored latent image.  
PSNR=29.34

**FIGURE 2:** Demonstration of intermediate representation, estimated kernel and recovered latent image in our process with blurry image as input. Restored image for Xu et al. is provided for comparison process.





(a) blurry input Image 1.

(b) our restored latent image and estimated kernel.



(c) blurry input Image 2.

(d) our restored latent image and estimated kernel.



(e) blurry input Image 3.

(f) our restored latent image and estimated kernel.

**FIGURE 3:** Experimental Results for Blurry Images.

Now, we go for the experimental results of images affected by both blur and noise, obtained by simulation based on the parameters and conditions defined in the beginning of this section. Wiener filtering has been a classic method used commonly in image denoising field [24]. The results by simulation of our method using directional filters for noise handling are given in Fig. 4, along with the results using Wiener filter proposed by Jin et al. [24], for comparison process. It can be seen that directional filtering produces much better visual quality images compared to Wiener filtering in all cases. It produces images with quality that is very comparable to that of the results obtained without noise, inspite of the presence of noise. Comparison of estimated kernels with ground truth kernels for two of the test images is shown in Fig. 5. It can be seen that the estimated kernel is indeed very much closer to the ground truth. Table 1 shows the PSNR values of the experimental results obtained for blurry images as well as blurry & noisy images equipped with noise handling. The last two columns of the table shows the comparative performance evaluation of results obtained by our method and those obtained by incorporating denoising proposed by Jin et al. [24] into the  $L_0$  deblurring process with a standard non-blind deconvolution proposed by Xu et al. [8]. Our method is seen to produce good visual quality results with high

improvement of PSNR values even in the presence of noise. Most of the existing methods fail to produce such high PSNR values without the use of explicit edge prediction steps like shock filter, in the presence of noise.



(a)restored latent image using Wiener filtering for blurry and noisy Image 1.

(b)restored latent image using directional filtering for blurry and noisy Image 1.



(c)restored latent image using Wiener filtering for blurry and noisy Image 2.

(d)restored latent image using directional filtering for blurry and noisy Image 2.



(e)restored latent image using Wiener filtering for blurry and noisy Image 3.

(f)restored latent image using directional filtering for blurry and noisy Image 3.

**FIGURE 4:** Experimental results of our method and Jin et al.[24] for blurry and noisy images - a comparison.



(a)Estimated kernels.



(b)Ground truths.

**FIGURE 5:** Comparison of estimated kernels with ground truth.

<b>Image</b>	<b>Input blurry image PSNR(dB)</b>	<b>L0 deblurred output for blurry image PSNR (dB)</b>	<b>L0 deblurred output for blurry &amp; noisy input after noise handling by Wiener filter(dB)</b>	<b>L0 deblurred output for blurry &amp; noisy input after noise handling by directional filter(dB)</b>
<i>Image 1</i>	20.33	30.20	28.12	29.25
<i>Image 2</i>	20.255	31.47	29.07	30.91
<i>Image 3</i>	27.33	32.81	30.51	32.61

**TABLE 1:** PSNR values of experimental results of our method for blurry images as well as for blurry & noisy images. Results of our method using directional filtering is compared to the results using Wiener filtering[24].

## 5. CONCLUSION

In this paper, we propose a new single image deblurring technique that is robust to noise unlike standard deblurring methods. Our method uses directional filtering for noise handling which does not affect the blur information and the kernel estimation process significantly in an adverse manner. A loss function approximating L0 cost is used as a prior for regularization in the objective function, which produces an unnatural sparse representation that benefits kernel estimation and optimization processes. A simple method is introduced in the final latent image restoration step to obtain a better quality image with much finer details and lesser artifacts. The method is very effective in handling blurry & noisy images compared to the existing deblurring techniques which deteriorates in performance when noise is present. As a future scope, the method can be extended to handle non-uniform blur in presence of noise.

## 6. REFERENCES

- [1] D. Kundur and D. Hatzinakos. "Blind image deconvolution", IEEE Signal Processing Magazine, 1996.
- [2] A. Levin, Y. Weiss, F. Durand and W. T. Freeman. "Understanding and evaluating blind deconvolution algorithms." In CVPR,2009, pp.1964–1971.
- [3] R. Fergus, B. Singh, A. Hertzmann, S. T. Roweis and W. T. Freeman." Removing camera shake from a single photograph." ACM Transactions on Graphics (SIGGRAPH ASIA), vol. 28 no.5, p. article no. 787–794, 2006.
- [4] Q. Shan, J. Jia, and A. Agarwala. "High-quality motion deblurring from a single image."ACM Transactions on Graphics (SIGGRAPH ASIA),vol. 27(3),2008.
- [5] J. H. Money and S. H. Kang. "Total variation minimizing blind deconvolution with shock filter reference." Image and Vision Computing, 26(2):302–314, 2008.

- [6] S. Cho and S. Lee. "Fast motion deblurring." ACM Transactions on Graphics (SIGGRAPH ASIA), vol. 28, no. 5, p. article no. 145, Dec. 2009.
- [7] D. Krishnan, T. Tay, and R. Fergus. "Blind deconvolution using a normalized sparsity measure." In CVPR, 2011, pp. 233–240.
- [8] L. Xu, S. Zheng and J. Jia. "Unnatural  $l_0$  sparse representation for natural image deblurring." In CVPR, 2013, pp. 1107–1114.
- [9] R. Koehler, M. Hirsch, S. Harmeling, B. Mohler and B. Scholkopf. "Recording and playback of camera shake: benchmarking blind deconvolution with a real-world database." In ECCV, 2012, pp. 27–40.
- [10] A. Levin, Y. Weiss, F. Durand, and W. T. Freeman. "Efficient marginal likelihood optimization in blind deconvolution." In CVPR2011, pp. 2657–2664.
- [11] A. Buades, B. Coll and J. Morel. "A non-local algorithm for image denoising." CVPR, 2005, pp. 60-65.
- [12] L. Zhang, A. Deshpande and X. Chen. "Denoising vs. deblurring: Hdr imaging techniques using moving cameras." In CVPR, 2010 pp. 522-529.
- [13] L. Zhong, S. Cho, D. Metaxas, S. Paris, and J. Wang. "Handling noise in single image deblurring using directional filters", In CVPR, 2013, pp. 612–619.
- [14] L. Xu and J. Jia. "Two-phase kernel estimation for robust motion deblurring", ECCV, 2010, pp. 157–170.
- [15] L. Xu, Q. Yan, Y. Xia and J. Jia. "Structure extraction from texture via relative total variation." ACM Transactions on Graphics (SIGGRAPH ASIA), vol. 31(6), 2012.
- [16] J. Jia. "Single image motion deblurring using transparency." In CVPR, 2007, pp. 1-8.
- [17] N. Joshi, R. Szeliski and D. J. Kriegman. "PSF estimation using sharp edge prediction." In CVPR, 2008, pp. 1-8.
- [18] T. S. Cho, S. Paris, B. K. P. Horn and W. T. Freeman. "Blur kernel estimation using the radon transform." In CVPR, 2011, pp. 241–248.
- [19] M. Hirsch, C. J. Schuler, S. Harmeling and B. Scholkopf. "Fast removal of non-uniform camera shake." In ICCV, 2011, pp. 463–470.
- [20] A. Buades, C. B. and J.-M. Morel. "The stair casing effect in neighborhood filters and its solution." IEEE Transaction on Image Processing, vol. 15, pp. 1499-1505, 2006.
- [21] D. Krishnan and R. Fergus. "Fast image deconvolution using hyper-laplacian priors." In NIPS, pp. 1033-1041, 2009.
- [22] Z. Hu, M. H. Yang, J. Pan and Z. Su. "Deblurring text images via  $L_0$  regularized intensity and gradient prior." In CVPR, 2014, pp. 2901-2908.
- [23] L. Xu, C. Lu, Y. Xu and J. Jia. "Image smoothing via  $l_0$  gradient minimization." ACM Transactions on Graphics (SIGGRAPH ASIA), vol. 30(6), 2011.

- [24] F. Jin, P. Fieguth, L. Winger and E. Jernigan. "Adaptive Wiener filtering of noisy images and image sequences." International Conference for Image Processing, IEEE, 2003, pp. 349-352.